From Trapped Atoms to Liberated Quarks

Thomas Schäfer

Department of Physics, North Carolina State University,
Raleigh, NC 27695
thomas_schaefer@ncsu.edu

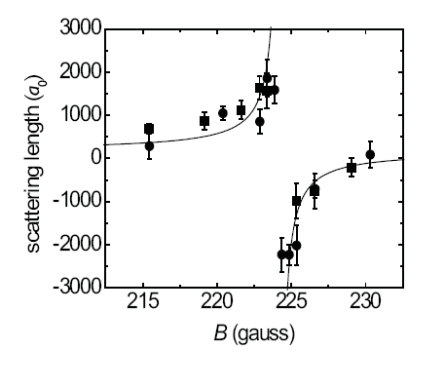
We discuss some aspects of cold atomic gases in the unitarity limit that are of interest in connection with the physics of dense hadronic matter. We consider, in particular, the equation of state at zero temperature, the magnitude of the pairing gap, and the phase diagram at non-zero polarization.

1. Introduction

The QCD phase diagram contains several strongly interacting quantum gases or liquids. Experiments at the Relativistic Heavy Ion Collider (RHIC) indicate that at temperatures close to the critical temperature T_c the quark gluon plasma is strongly interacting. The strongly interacting plasma (sQGP) is characterized by a very small viscosity to entropy ratio and by its large opacity for high energy jets ¹. In the opposite regime of large baryon density and small temperature the phase diagram features several strongly interacting quantum liquids. Electrically neutral matter at very low density contains mostly neutrons. Dilute neutron matter has positive pressure and is stable even at very low density. However, the neutron-neutron scattering length is very large and as a consequence neutron matter is strongly correlated even if the density is low ². At densities on the order of several times nuclear matter density hadronic matter undergoes a phase transition to color superconducting quark matter. At extremely large density this phase is weakly coupled, but at densities near the transition to nuclear matter the gap and the critical temperature are probably large ³.

There are many questions about strongly interacting phases of QCD that have attracted a lot of interest. Some of these questions are: What are the relevant degrees of freedom? Are quasi-particle pictures appropriate? What are the transport properties? Is it true that there is a universal bound on the viscosity, and is this bound saturated in any of the strongly interacting phases of QCD?

In this contribution we shall study a simpler system in which many of the same questions can be addressed. We consider a cold, dilute gas of fermionic atoms in which the scattering length a of the atoms can be controlled experimentally.



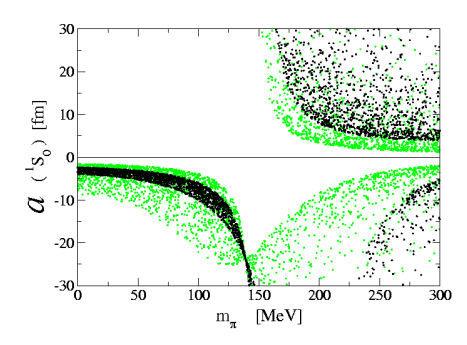


Fig. 1. The left panel shows the scattering length of 40 K Atoms as a function of the magnetic field near a Feshbach resonance, from Regal (2005). The right panel shows the nucleon-nucleon scattering length in the $^{1}S_{0}$ channel as a function of the pion mass. The scatter plot indicates the uncertainty due to higher order terms in the chiral effective lagrangian. Figure from Savage and Beane (2003).

These systems can be realized in the laboratory using Feshbach resonances, see 4 for a review. A small negative scattering length corresponds to a weak attractive interaction between the atoms. This case is known as the BCS limit. As the strength of the interaction increases the scattering length becomes larger. It diverges at the point where a bound state is formed. The point $a=\infty$ is called the unitarity limit, since the scattering cross section saturates the s-wave unitarity bound $\sigma=4\pi/k^2$. On the other side of the resonance the scattering length is positive. In the BEC limit the interaction is strongly attractive and the fermions form deeply bound molecules.

A dilute gas of fermions in the unitarity limit is a strongly coupled quantum liquid that exhibits many interesting properties. On a qualitative level these properties are of interest in connection with other strongly interacting field theories. The unitarity limit is also quantitatively relevant to the physics of dilute neutron matter. The neutron-neutron scattering length is $a_{nn}=-18$ fm and the effective range is $r_{nn}=2.8$ fm. This means that there is a range of densities for which the interparticle spacing is large compared to the effective range but small compared to the scattering length. It is interesting to note that the neutron scattering length depends on the quark masses in a way that is very similar to the dependence of atomic scattering lengths on the magnetic field near a Feshbach resonance 5 , see Fig. 1.

2. Universal equation of State

2.1. Cold Atomic Gases

We first consider the equation of state of cold fermions in the unitarity limit. We are interested in the limit $(k_F a) \to \infty$ and $(k_F r) \to 0$, where k_F is the Fermi

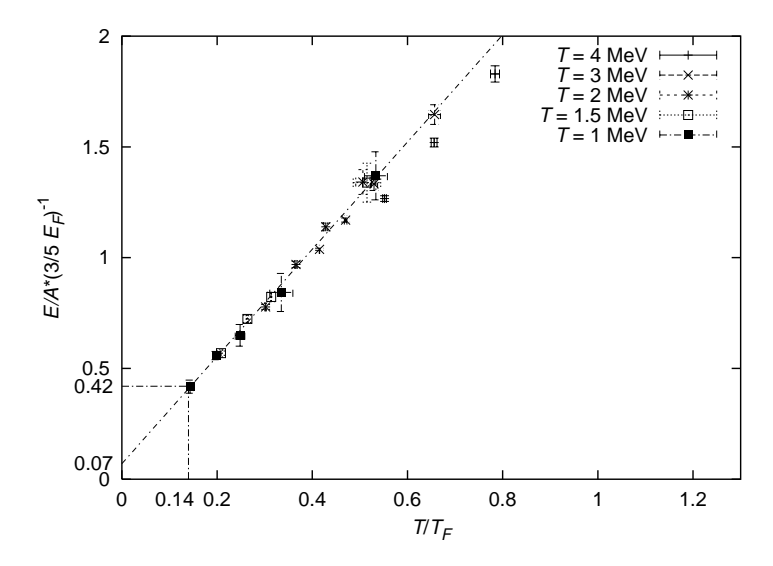


Fig. 2. Lattice results for the energy per particle of a dilute Fermi gas from Lee & Schäfer (2005). We show the energy per particle in units of $3E_F/5$ as a function of temperature in units of T_F .

momentum, a is the scattering length and r is the effective range. From dimensional analysis it is clear that the energy per particle has to be proportional to energy per particle of a free Fermi gas at the same density

$$\frac{E}{A} = \xi \left(\frac{E}{A}\right)_0 = \xi \frac{3}{5} \left(\frac{k_F^2}{2m}\right),\tag{1}$$

where k_F is the Fermi momentum. The calculation of the dimensionless quantity ξ is a non-perturbative problem. We shall tackle this problem using a combination of effective field theory and lattice field theory methods. We first observe that in the low density limit the details of the interaction are not important. The physics of the unitarity limit is captured by an effective lagrangian of point-like fermions interacting via a short-range interaction. The lagrangian is

$$\mathcal{L} = \psi^{\dagger} \left(i \partial_0 + \frac{\nabla^2}{2m} \right) \psi - \frac{C_0}{2} \left(\psi^{\dagger} \psi \right)^2, \tag{2}$$

where m is the mass of the fermion and C_0 is the strength of the four-fermion interaction. In the weak coupling limit C_0 is related to the scattering length by $C_0 = 4\pi a/m$.

If the scattering length is small then the energy of the many body system can be computed as a perturbative expansion in $(k_F a)$. If $(k_F a)$ is large we have to rely on numerical simulations. The partition function can be written as 6

$$Z = \int DsDcDc^* \exp\left[-S\right],\tag{3}$$

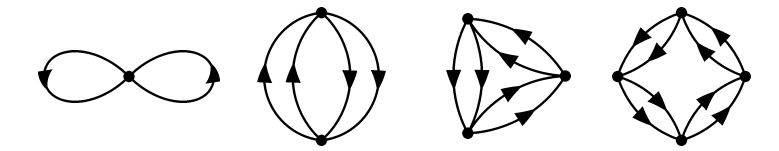


Fig. 3. Particle-particle ladder diagrams.

where S is a discretized euclidean action

$$S = \sum_{\vec{n},i} \left[e^{-\mu\alpha_t} c_i^*(\vec{n}) c_i'(\vec{n} + \hat{0}) - e^{\sqrt{-C_0\alpha_t}s(\vec{n}) + \frac{C_0\alpha_t}{2}} (1 - 6h) c_i^*(\vec{n}) c_i'(\vec{n}) \right] - h \sum_{\vec{n},l_s,i} \left[c_i^*(\vec{n}) c_i'(\vec{n} + \hat{l}_s) + c_i^*(\vec{n}) c_i'(\vec{n} - \hat{l}_s) \right] + \frac{1}{2} \sum_{\vec{n}} s^2(\vec{n}).$$
(4)

Here, s is a Hubbard-Stratonovich field, c is a Grassmann field, α_t is the ratio of the temporal and spatial lattice spacings and $h=\alpha_t/(2m)$. The sums are over spin labels i, lattice sites \vec{n} , and spatial unit vectors \hat{l} . $\hat{0}$ is a temporal unit vector. Note that for $C_0<0$ the action is real and standard Monte Carlo simulations are possible. Results in the unitarity limit are shown in Fig. 2. From these simulations we concluded that $\xi=(0.09-0.42)$. Lee performed canonical simulations at T=0 and obtained $^7\xi=0.25$. Green Function Monte Carlo calculations give $^8\xi=0.44$, and finite temperature lattice simulations have been extrapolated to T=0 to yield similar results 9,10 .

It is also interesting to find analytical approaches to the equation of state in the unitarity limit. Since the two-body interaction is large it is natural to begin with the sum of all two-body diagrams, see Fig. 3. This sum gives ¹¹

$$\frac{E}{N} = \frac{k_F^2}{2M} \left\{ \frac{3}{5} + \frac{2(k_F a)/(3\pi)}{1 - \frac{6}{35\pi}(11 - 2\log(2))(k_F a)} \right\}.$$
 (5)

from which we deduce $\xi \simeq 0.32$. This is reasonably close to the numerical results, but since the system is strongly correlated there is no obvious reason to restrict ourselves to two-body ladders. We have recently studied the possibility that equ. (5) can be justified as the leading term in an expansion in 1/d, where d is the number of spatial dimensions 12,11 . This approach appears promising, but 1/d corrections have not been worked out yet. In order to obtain a smooth $d \to \infty$ limit the coupling constant has to be scaled in a specific way. Nussinov & Nussinov observed that if the limit $a \to \infty$ is taken first then the point d=4 is special 13 . In d=4 the two-body wave function at $a=\infty$ has a $1/r^2$ behavior and the normalization is concentrated near the origin. This implies that the many body system is equivalent to a gas of non-interacting bosons and $\xi(d=4)=0$. Nishida and Son computed ξ in d=3 using an expansion around this limit. At next-to-leading order they find 14 $\xi=0.475$.

2.2. Strongly Coupled Gauge Theory

In connection with the RHIC program we are interested in understanding the quark gluon plasma in the vicinity of the critical temperature. From lattice simulations we know that the energy density quickly reaches about 80% of the ideal gas value, and that this ratio is only very weakly temperature dependent on temperature for $T > 2T_c$. This behavior can be understood in hard thermal loop resummed perturbation theory ¹⁵. In this framework the degrees of freedom are dressed quasiquarks and quasi-gluons, and these quasi-particles are weakly interacting.

Transport properties of the plasma indicate that this may not be the end of the story. If quasi-particles are indeed weakly interacting then it is hard to see how the viscosity can be anomalously low or the opacity be very large. A complementary, strong coupling, calculation was performed in the strong coupling and large N_c limit of $\mathcal{N}=4$ SUSY Yang Mills theory. The calculation is based on the duality between the strongly coupled gauge theory and weakly coupled string theory on $AdS_5 \times S_5$ discovered by Maldacena ¹⁶. The correspondence can be extended to finite temperature. In this case the relevant configurations is an AdS_5 black hole. The temperature of the gauge theory is given by the Hawking temperature of the black hole, and the entropy is given by the Hawking-Beckenstein formula. The result is that the entropy density of the strongly coupled field theory is equal to 3/4 of the free field theory value ¹⁷. Clearly, the number 3/4 can be viewed as a gauge theory analog of the parameter ξ studied in the previous section. The remarkable result is that the gauge theory value is so close to one, so that based on the equation of state alone one cannot easily distinguish a strongly and a weakly coupled system.

3. Pairing

3.1. Cold Atomic Gases

At low temperature the atomic gas becomes superfluid. If the coupling is weak then the gap and the critical temperature can be calculated using BCS theory. The result

$$\Delta = \frac{8E_F}{(4e)^{1/3}e^2} \exp\left(-\frac{\pi}{2k_F|a|}\right),\tag{6}$$

where the factor $(4e)^{1/3}$ is the screening correction first computed by Gorkov et al. ¹⁸. Higher order corrections are suppressed by powers of $(k_F a)$. In BCS theory the critical temperature is given by $T_c = e^{\gamma} \Delta / \pi$. Clearly, the critical temperature grows with the scattering length. Naively extrapolating equ. (6) to the unitarity limit gives $T_c \simeq 0.28 E_F$. In the BEC limit the critical temperature is given by the Einstein result $T_c = 3.31 \rho^{2/3}/m$. Writing E_F in terms of the density this corresponds to $T_c \simeq 0.34 E_F$. Interactions between the bosons increase the critical temperature ¹⁹, $T_c = T_c^0 + O(a_B \rho^{1/3})$. Near the unitarity limit the boson scattering length a_B is proportional to the fermion scattering length 20 , $a_{BB} \simeq 0.6a$. These results suggests that the unitarity limit may correspond to the maximum possible value of T_c/E_F .

The value of T_c has been determined in a number of lattice calculations. A careful scaling analysis by Burovski et al. yields 10 $T_c = 0.152(7)E_F$. Earlier determinations of T_c can be found in 21,9 . A direct calculation of the pairing gap at zero temperature using Green Function Monte Carlo methods gives 22 $\Delta = 0.54E_F$.

3.2. Color Superconductivity

Pairing also takes place in the high density, low temperature phase of QCD. At asymptotically large density the attraction is due to one-gluon exchange between fermions with opposite momenta and anti-symmetric spin, color and flavor wave functions. In this limit the pairing gap is given by 23,24

$$\Delta = 2\Lambda_{BCS} \exp\left(-\frac{\pi^2 + 4}{8}\right) \exp\left(-\frac{3\pi^2}{\sqrt{2}g}\right). \tag{7}$$

where g is the running coupling constant evaluated at the scale μ and $\Lambda_{BCS} = 256\pi^4(2/N_f)^{5/2}g^{-5}\mu$. Here, μ is the baryon chemical potential and N_F is the number of flavors. This result exhibits a non-BCS like dependence on the coupling constant which is related to the presence of unscreened magnetic gluon exchanges. The critical temperature is nevertheless given by the BCS result $T_c = e^{\gamma} \Delta/\pi$.

If the weak coupling limit the gap and the critical temperature are exponentially small. The ratio T_c/E_F increases with g and reaches a maximum of $T_c = 0.025E_F$ at g = 4.2. The maximum occurs at strong coupling and the result is not reliable. Using phenomenological interactions, or extrapolating the QCD Dyson-Schwinger equations into the strong coupling domain 25 , one finds critical temperatures as large as $T_c = 0.15E_F$. In connection with phenomenological applications to neutron stars and the physics of heavy ion collisions in the regime of the highest baryon densities it is very important to reduce the uncertainty in these estimates. One possibility is to use lattice studies of QCD-like theories in which the euclidean action remains positive at finite chemical potential. Examples are QCD with two colors and QCD at finite isospin density.

4. Stressed Pairing

4.1. Polarized Cold Atomic Gases

The superfluid state discussed in Sect. 3.1 involves equal numbers of spin up and spin down fermions. One aspect of the paired state that has attracted a lot of interest is the response of this system to a non-zero chemical potential coupled to the third component of spin, $\delta\mu = \mu_{\uparrow} - \mu_{\downarrow}$. A conjectured (and, most likely, oversimplified) phase diagram for a polarized gas is shown in Fig. 4. In the BEC limit the gas consists of tightly bound spin singlet molecules. Adding an extra up or down spin requires energy Δ . For $|\delta\mu| > \Delta$ the system is a homogeneous mixture of a Bose condensate and a fully polarized Fermi gas. One can show that in the dilute limit this mixture is stable with regard to phase separation ²⁶.

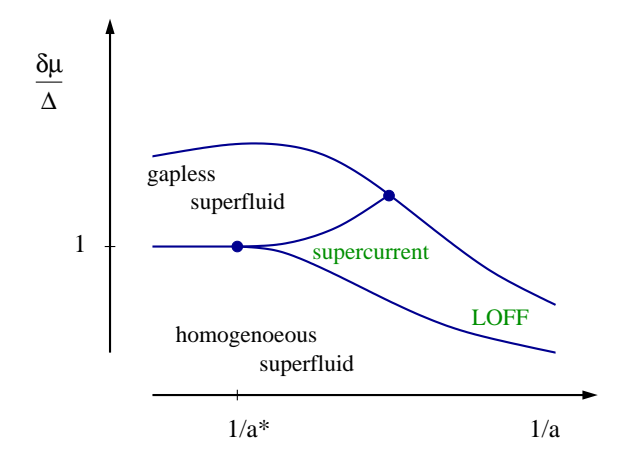


Fig. 4. Conjectured phase diagram for a polarized cold atomic Fermi gas as a function of the scattering length a and the difference in the chemical potentials $\delta\mu=\mu_{\uparrow}-\mu_{\downarrow}$, from Son & Stephanov (2005).

We can also analyze the system in the BCS limit. This analysis goes back to the work of Larkin, Ovchninikov, Fulde and Ferell (LOFF) ^{27,28}, see the review ²⁹. We first consider homogeneous solutions to the BCS gap equation for $\delta \mu \neq 0$. In the regime $\delta\mu < \Delta_0$ where $\Delta_0 = \Delta(\delta\mu = 0)$ the gap equation has a solution with gap parameter $\Delta = \Delta_0$. This solution is stable if $\delta \mu < \Delta_0/\sqrt{2}$ but only meta-stable in the regime $\Delta_0/\sqrt{2} < \delta\mu < \Delta_0$. The BCS solution has vanishing polarization. The transition to a polarized normal phase is first order, and systems at intermediate polarization correspond to mixed phases.

LOFF studied whether it is possible to find a stable solution in which the gap has a spatially varying phase

$$\Delta(\vec{x}) = \Delta e^{2i\vec{q}\cdot\vec{x}}.$$
 (8)

This solution exists in the LOFF window $\delta\mu_1 < \delta\mu < \delta\mu_2$ with $\delta\mu_1 = \Delta_0/\sqrt{2} \simeq$ $0.71\Delta_0$ and $\delta\mu_2 \simeq 0.754\Delta_0$. The LOFF momentum q depends on $\delta\mu$. Near $\delta\mu_2$ we have $qv_F \simeq 1.2\delta\mu$, where v_F is the Fermi velocity. The gap Δ goes to zero near $\delta\mu_2$ and reaches $\Delta \simeq 0.25\Delta_0$ at $\delta\mu_1$.

These results suggest that at some point on the phase diagram between the BEC and BCS limits the homogeneous superfluid becomes unstable with respect to the formation of a non-zero supercurrent $\nabla \varphi$, where φ is the phase of the condensate. We can study this question using the effective lagrangian

$$\mathcal{L} = \psi^{\dagger} \left(i \partial_0 - \epsilon(-i\vec{\partial}) - i(\vec{\partial}\varphi) \cdot \frac{\overleftrightarrow{\partial}}{2m} \right) \psi + \frac{f_t^2}{2} \dot{\varphi}^2 - \frac{f^2}{2} (\vec{\partial}\varphi)^2. \tag{9}$$

Here, ψ describes a fermion with dispersion law $\epsilon(\vec{p})$ and φ is the superfluid Goldstone mode. The low energy parameters f_t and f are related to the density and the velocity of sound. The p-wave coupling of the fermions to the Goldstone boson is governed by the U(1) symmetry of the theory.

Setting up a current $\vec{v}_s = \vec{\partial} \varphi/m$ requires energy $f^2 m^2 v_s^2/2$. The contribution from fermions can be computed using the fermion dispersion law in the presence of a non-zero current

$$\epsilon_v(\vec{p}) = \epsilon(\vec{p}) + \vec{v}_s \cdot \vec{p} - \delta\mu. \tag{10}$$

The total free energy is

$$F(v_s) = \frac{1}{2}nmv_s^2 + \int \frac{d^3p}{(2\pi)^3} \,\epsilon_v(\vec{p})\Theta\left(-\epsilon_v(\vec{p})\right),\tag{11}$$

where n is the density and we have used $f^2 = n/m$. Son and Stephanov noticed that the stability of the homogeneous phase depends crucially on the nature of the dispersion law $\epsilon(p)$. For small momenta we can write $\epsilon(p) \simeq \epsilon_0 + \alpha p^2 + \beta p^4$. In the BEC limit $\alpha > 0$ and the minimum of the dispersion curve is at p = 0 while in the BCS limit $\alpha < 0$ and the minimum is at $p \neq 0$. In the latter case the density of states on the Fermi surface is finite and the system is unstable with respect to the formation of a non-zero current. On the other hand, if the minimum of the dispersion curve is at zero, then the density of states vanishes and there is no instability. As a consequence there is a critical point along the BEC-BCS line at which the instability will set in.

Clearly, the LOFF solution is of the same type as the supercurrent state. The difference is that in the supercurrent state the current is much smaller than the gap, $v_F(\nabla\varphi) \ll \Delta$, while in the LOFF phase $v_F(\nabla\varphi) > \Delta$ (and $v_F(\nabla\varphi) \gg \Delta$ near $\delta\mu_2$). In the supercurrent state the Fermi surface is mostly gapped but a small shell near one of the pole caps is ungapped. In the weakly coupled LOFF state there are gapless excitations over most of the Fermi surface but pairing takes place near two rings on the northern and southern hemisphere.

4.2. CFL Phase at Non-zero Strange Quark Mass

The exact nature of the color superconducting phase in QCD depends on the baryon chemical potential, the number of quark flavors and on their masses. If the baryon chemical is much larger than the quark masses then the ground state of QCD with three flavors is the color-flavor-locked (CFL) phase. The CFL phase is characterized by the pair condensate 30

$$\langle \psi_i^a C \gamma_5 \psi_j^b \rangle = (\delta_i^a \delta_j^b - \delta_j^a \delta_i^b) \phi. \tag{12}$$

This condensate leads to a gap in the excitation spectrum of all fermions and completely screens the gluonic interaction. Both the chiral $SU(3)_L \times SU(3)_R$ and color SU(3) symmetry are broken, but a vector-like SU(3) flavor symmetry remains unbroken.

In the real world the strange quark mass is not equal to the masses of the up and down quark and flavor symmetry is broken. At high baryon density the effect of the quark masses is governed by the shift $\mu_q = m_q^2/(2\mu)$ of the Fermi energy due to the quark mass. This implies that flavor symmetry breaking becomes more important as the density is lowered. Clearly, the most important effect is due to the strange quark mass. There are two scales that are important in relation to μ_s . The first is the mass of the lightest strange Goldstone boson, the kaon, and the second is the gap Δ for fermionic excitations. When μ_s becomes equal to m_K the CFL phase undergoes a transition to a phase with kaon condensation ³¹. In the following we shall study the phase structure near $\mu_s \sim \Delta$.

Our starting point is the effective theory of the CFL phase derived in ^{32,33}. The effective lagrangian contains Goldstone boson fields Σ and baryon fields N. The meson fields arise from chiral symmetry breaking in the CFL phase. The leading terms in the effective theory are

$$\mathcal{L} = \frac{f_{\pi}^2}{4} \operatorname{Tr} \left(\nabla_0 \Sigma \nabla_0 \Sigma^{\dagger} - v_{\pi}^2 \vec{\nabla} \Sigma \vec{\nabla} \Sigma^{\dagger} \right), \tag{13}$$

where f_{π} is the pion decay constant. The chiral field transforms as $\Sigma \to L\Sigma R^{\dagger}$ under chiral transformations $(L,R) \in SU(3)_L \times SU(3)_R$. Baryon fields originate from quark-hadron complementarity ³⁴. The effective lagrangian is

$$\mathcal{L} = \operatorname{Tr}\left(N^{\dagger}iv^{\mu}D_{\mu}N\right) - D\operatorname{Tr}\left(N^{\dagger}v^{\mu}\gamma_{5}\left\{\mathcal{A}_{\mu},N\right\}\right) - F\operatorname{Tr}\left(N^{\dagger}v^{\mu}\gamma_{5}\left[\mathcal{A}_{\mu},N\right]\right) + \frac{\Delta}{2}\left\{\left(\operatorname{Tr}\left(N_{L}N_{L}\right) - \left[\operatorname{Tr}\left(N_{L}\right)\right]^{2}\right) - \left(\operatorname{Tr}\left(N_{R}N_{R}\right) - \left[\operatorname{Tr}\left(N_{R}\right)\right]^{2}\right) + h.c.\right\}, (14)$$

where $N_{L,R}$ are left and right handed baryon fields in the adjoint representation of flavor SU(3), $v^{\mu}=(1,\vec{v})$ is the Fermi velocity, and Δ is the superfluid gap. We can think of N as being composed of a quark and a diquark field, $N_L \sim q_L \langle q_L q_L \rangle$. The interaction of the baryon field with the Goldstone bosons is dictated by chiral symmetry. The covariant derivative is given by $D_{\mu}N = \partial_{\mu}N + i[\mathcal{V}_{\mu}, N]$. The vector and axial-vector currents are

$$V_{\mu} = -\frac{i}{2} \left\{ \xi \partial_{\mu} \xi^{\dagger} + \xi^{\dagger} \partial_{\mu} \xi \right\}, \qquad \mathcal{A}_{\mu} = -\frac{i}{2} \xi \left(\partial_{\mu} \Sigma^{\dagger} \right) \xi, \tag{15}$$

where ξ is defined by $\xi^2 = \Sigma$. The low energy constants f_{π}, v_{π}, D, F can be calculated in perturbative QCD. Symmetry arguments can be used to determine the leading mass terms in the effective lagrangian. Bedaque and Schäfer observed that $X_L = MM^{\dagger}/(2p_F)$ and $X_R = M^{\dagger}M/(2p_F)$ act as effective chemical potentials and enter the theory like the temporal components of left and right handed flavor gauge fields ³¹. We can make the effective lagrangian invariant under this symmetry by introducing the covariant derivatives

$$D_0 N = \partial_0 N + i [\Gamma_0, N], \quad \Gamma_0 = -\frac{i}{2} \left\{ \xi \left(\partial_0 + i X_R \right) \xi^{\dagger} + \xi^{\dagger} \left(\partial_0 + i X_L \right) \xi \right\},$$
(16)
$$\nabla_0 \Sigma = \partial_0 \Sigma + i X_L \Sigma - i \Sigma X_R.$$
(17)

Using equ. (14-16) we can calculate the dependence of the gap in the fermion spectrum on the strange quark mass. For $m_s = 0$ there are 8 quasi-particles with gap Δ and one quasi-particle with gap 2Δ . As m_s increases some of the gaps

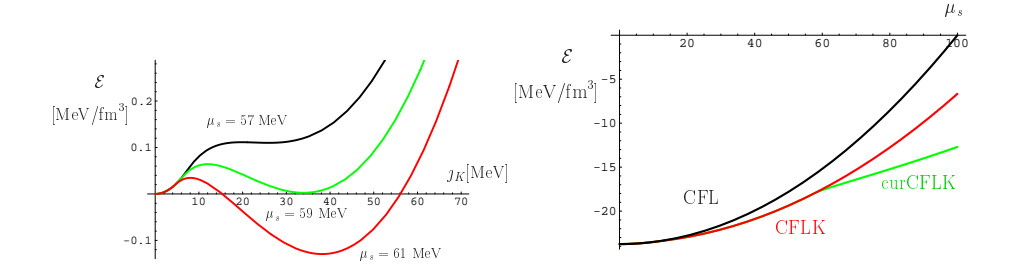


Fig. 5. Left panel: Energy density as a function of the current j_K for several different values of $\mu_s = m_s^2/(2p_F)$ close to the phase transition. Right panel: Ground state energy density as a function of μ_s . We show the CFL phase, the kaon condensed CFL (KCFL) phase, and the supercurrent state (curKCFL).

decrease. In the K^0 condensed phase the gap of the lowest mode is approximately given by $\Delta = \Delta_0 - 3\mu_s/4$ where $\mu_s = m_s^2/(2p_F)$ and Δ_0 is the gap in the chiral limit.

For $\mu_s \sim 4\Delta_0/3$ the system contains low energy fermions derivatively coupled to Goldstone bosons. The situation is essentially equivalent to the cold atomic system studied in the previous section. The main difference is that in the CFL phase there are many more currents that can appear. In the K^0 condensed phase the natural ansatz is a hypercharge current carried by the kaon field. We take $\xi(x) = U(x)\xi_{K^0}$ where ξ_{K^0} is the K^0 background, U(x) is a hypercharge transformation and $\vec{\jmath}_K = iU^{\dagger}\vec{\nabla}U$ is the kaon current. The dispersion relation of the lowest mode is 35,36

$$\omega_l = \Delta_0 + \frac{l^2}{2\Delta_0} - \frac{3}{4}\mu_s - \frac{1}{4}\vec{v} \cdot \vec{j}_K, \tag{18}$$

where l is the momentum relative to the Fermi surface. The energy relative to the CFL phase is the kinetic energy of the current plus the energy of occupied gapless modes

$$\mathcal{E} = \frac{1}{2} v_{\pi}^2 f_{\pi}^2 \vec{j}_K^2 + \frac{\mu^2}{\pi^2} \int dl \int \frac{d\Omega}{4\pi} \,\omega_l \theta(-\omega_l). \tag{19}$$

The energy functional can develop a minimum at non-zero j_K because the current lowers the energy of the fermions near one of the pole caps on the Fermi surface. Introducing the dimensionless variables $x = j_K/(a\Delta)$ and $h = (3\mu_s - 4\Delta)/(a\Delta)$ we can write

$$\mathcal{E} = Cf_h(x), \quad f_h(x) = x^2 - \frac{1}{x} \left[(h+x)^{5/2} \Theta(h+x) - (h-x)^{5/2} \Theta(h-x) \right],$$
 (20)

where C and a are numerical constants. The functional given in equ. (20) was analyzed in 37,35,36 , see Fig. 5. There is a critical chemical potential $\mu_s = (4/3 + ah_{crit}/3)\Delta$ above which the groundstate contains a non-zero supercurrent j_K . This current is canceled by a backflow of gapless fermions. The Goldstone current phase

is analogous to the supercurrent state in cold atomic systems, and to p-wave pion condensates in nuclear matter.

The Goldstone current phase in pure CFL matter, without an s-wave kaon condensate, was analyzed by Gerhold and Schäfer ³⁸. In that case the structure of the current is different, but the energy functional and the nature of the instability are very similar. Gerhold and Schäfer showed, in particular, that the magnetic screening masses in the Goldstone boson current phase are real. Near the onset of the instability the current is small compared to the gap, but the current grows with the mismatch μ_s . Once the current becomes comparable to the gap it may be more appropriate to characterize the system as a LOFF state ³⁹.

5. Outlook

There are many questions about cold fermion gases in the unitarity limit, and about their relevance to strongly interacting hadronic matter, that remain to be resolved. The unitarity limit is most directly connected with the physics of dilute neutron matter. In neutron matter the scattering length is not exactly infinite, and the effective range is not zero. It is clearly important to understand how corrections due to the finite scattering length and effective range affect the equation of state and other observables.

There is a great deal of experimental effort devoted to the study of polarized fermionic gases. Mixed phases of superfluids and polarized normal fluids have been observed ⁴⁰, but so far none of the predicted inhomogeneous or gapless superfluids have been experimentally detected. Finally, much work remains to done with regard to the transport properties of cold fermionic gases. We would like to understand, both theoretically and experimentally, how the shear viscosity depends on the temperature and the scattering length. Damping of collective oscillations of trapped fermions has been observed experimentally ⁴¹, but the damping coefficients have not been related to transport properties of the bulk system.

Acknowledgments: The work described in this contribution was done in collaboration with S. Cotanch, A. Gerhold, C.-W. Kao, A. Kryjevski and D. Lee. This work is supported in part by the US Department of Energy grant DE-FG-88ER40388.

References

- 1. I. Arsenne et al. [Brahms], B. Back et al. [Phobos], K. Adcox et al. [Phenix], J. Adams et al. [Star], "First Three Years of Operation of RHIC", Nucl. Phys. A757, 1-183
- 2. B. Friedman and V. R. Pandharipande, Nucl. Phys. A 361, 502 (1981); S. Y. Chang et al., Nucl. Phys. A 746, 215 (2004) [nucl-th/0401016]; G. A. Baker, Phys. Rev. C 60, 054311 (1999)
- 3. R. Rapp, T. Schäfer, E. V. Shuryak and M. Velkovsky, Annals Phys. 280, 35 (2000) [hep-ph/9904353]; M. G. Alford, K. Rajagopal and F. Wilczek, Phys. Lett. B 422, 247 (1998) [hep-ph/9711395].
- 4. C. Regal, Ph. D. Thesis, University of Colorado (2005), cond-mat/0601054.

- 5. S. R. Beane and M. J. Savage, Nucl. Phys. A 717, 91 (2003) [nucl-th/0208021].
- D. Lee and T. Schäfer, Phys. Rev. C 72, 024006 (2005) [nucl-th/0412002]; Phys. Rev. C 73, 015201 (2006) [nucl-th/0509017]; Phys. Rev. C 73, 015202 (2006) [nucl-th/0509018].
- 7. D. Lee, Phys. Rev. B **73**, 115112 (2006) [cond-mat/0511332].
- J. Carlson, J. J. Morales, V. R. Pandharipande and D. G. Ravenhall, Phys. Rev. C 68, 025802 (2003) [nucl-th/0302041].
- A. Bulgac, J. E. Drut and P. Magierski, Phys. Rev. Lett. 96, 090404 (2006) [cond-mat/0505374].
- E. Burovski, N. Prokof'ev, B. Svistunov, M. Troyer, Phys. Rev. Lett. 96, 160402 (2006) [cond-mat/0602224].
- T. Schäfer, C. W. Kao and S. R. Cotanch, Nucl. Phys. A 762, 82 (2005) [nucl-th/0504088].
- 12. J. V. Steele, preprint, nucl-th/0010066.
- 13. Z. Nussinov and S. Nussinov, preprint, cond-mat/0410597.
- 14. Y. Nishida and D. T. Son, preprint, cond-mat/0604500.
- J. P. Blaizot, E. Iancu and A. Rebhan, Thermodynamics of the high-temperature quark gluon plasma, in Quark Gluon Plasma 3, R. Hwa, X.-N. Wang, eds., (2003) [hep-ph/0303185].
- 16. J. M. Maldacena, Adv. Theor. Math. Phys. 2, 231 (1998) [hep-th/9711200].
- S. S. Gubser, I. R. Klebanov and A. A. Tseytlin, Nucl. Phys. B 534, 202 (1998) [hep-th/9805156].
- 18. L. P. Gorkov and T. K. Melik-Barkhudarov, Sov. Phys. JETP 13, 1018 (1961).
- M. Holzmann, G. Baym, J.-P. Blaizot and F. Laloe, Phys. Rev. Lett. 87, 120403 (2001).
- D. S. Petrov, C. Salomon, G. V. Shlyapnikov, Phys. Rev. A 71, 012708 (2005) [cond-mat/0407579].
- 21. M. Wingate, preprint, hep-lat/0409060.
- J. Carlson, S.-Y. Chang, V. R. Pandharipande, and K. E. Schmidt, Phys. Rev. Lett. 91, 050401, (2003).
- 23. D. T. Son, Phys. Rev. **D59**, 094019 (1999) [hep-ph/9812287].
- T. Schäfer and F. Wilczek, Phys. Rev. D60, 114033 (1999) [hep-ph/9906512];
 R. D. Pisarski and D. H. Rischke, Phys. Rev. D61, 074017 (2000) [nucl-th/9910056];
 D. K. Hong, V. A. Miransky, I. A. Shovkovy and L. C. Wijewardhana, Phys. Rev. D61, 056001 (2000) [hep-ph/9906478];
 W. E. Brown, J. T. Liu and H. c. Ren, Phys. Rev. D 61, 114012 (2000) [hep-ph/9908248].
- 25. D. Nickel, J. Wambach and R. Alkofer, preprint, hep-ph/0603163.
- L. Viverit, C. J. Pethick, H. Smith, Phys. Rev. A61 053605 (2000) [cond-mat/9911080].
- A. I. Larkin and Yu. N. Ovchinikov, Zh. Eksp. Theor. Fiz. 47, 1136 (1964); engl. translation: Sov. Phys. JETP 20, 762 (1965).
- 28. P. Fulde and A. Ferrell, Phys. Rev. **145**, A550 (1964).
- 29. R. Casalbuoni and G. Nardulli, Rev. Mod. Phys. **76**, 263 (2004) [hep-ph/0305069].
- M. Alford, K. Rajagopal and F. Wilczek, Nucl. Phys. B537, 443 (1999) [hep-ph/9804403].
- 31. P. F. Bedaque and T. Schäfer, Nucl. Phys. A697, 802 (2002) [hep-ph/0105150].
- 32. R. Casalbuoni and D. Gatto, Phys. Lett. **B464**, 111 (1999) [hep-ph/9908227].
- 33. A. Kryjevski and T. Schäfer, Phys. Lett. B **606**, 52 (2005) [hep-ph/0407329].; A. Kryjevski and D. Yamada, Phys. Rev. D **71**, 014011 (2005) [hep-ph/0407350].
- 34. T. Schäfer and F. Wilczek, Phys. Rev. Lett. 82, 3956 (1999) [hep-ph/9811473].

- 35. A. Kryjevski, preprint, hep-ph/0508180.
- 36. T. Schäfer, Phys. Rev. Lett. **96**, 012305 (2006) [hep-ph/0508190].
- 37. D. T. Son and M. A. Stephanov, preprint, cond-mat/0507586.
- 38. A. Gerhold and T. Schäfer, preprint, hep-ph/0603257.
- 39. R. Casalbuoni, R. Gatto, N. Ippolito, G. Nardulli and M. Ruggieri, Phys. Lett. B $\bf 627,\,89$ (2005) [hep-ph/0507247]; M. G. Alford, J. A. Bowers and K. Rajagopal, Phys. Rev. D 63, 074016 (2001) [hep-ph/0008208].
- 40. M. W. Zwierlein, C. H. Schunck, A. Schirotzek, W. Ketterle, preprint, condmat/0605258.
- 41. J. Kinast, A. Turlapov, J. E. Thomas, Phys. Rev. A 70, 051401(R) (2004) [condmat/0409283].